Z. Angew. Math. Phys. (2018) 69:43

0044-2275/18/020001-18
published online March 21, 2018
https://doi.org/10.1007/s00033-018-0939-4

Zeitschrift für angewandte Mathematik und Physik ZAMP

Time-dependent electrophoresis of a dielectric spherical particle embedded in Brinkman medium

E. I. Saad and M. S. Faltas

Abstract. An expression for electrophoretic apparent velocity slip in the time-dependent flow of an electrolyte solution saturated in a charged porous medium within an electric double layer adjacent to a dielectric plate under the influence of a tangential uniform electric field is derived. The velocity slip is used as a boundary condition to solve the electrophoretic motion of an impermeable dielectric spherical particle embedded in an electrolyte solution saturated in porous medium under the unsteady Darcy–Brinkman model. Throughout the system, a uniform electric field is applied and maintains with constant strength. Two cases are considered, when the electric double layer enclosing the particle is thin, but finite and when of a particle with a thick double layer. Expressions for the electrophoretic mobility of the particle as functions of the relevant parameters are found. Our results indicate that the time scale for the growth of mobility is significant and small for high permeability. Generally, the effect of the relaxation time for starting electrophoresis is negligible, irrespective of the thickness of the double layer and permeability of the medium. The effects of the elapsed time, permeability, mass density and Debye length parameters on the fluid velocity, the electrophoretic mobility and the acceleration are shown graphically.

Mathematics Subject Classification. 76S05, 76D07, 76W05.

Keywords. Brinkman equation, Time-dependent electrophoresis, Electrophoretic mobility.

1. Introduction

Electrophoresis phenomenon was noticed, for the first time, in the pioneering work of Reuss [1]. Electrophoresis is the motion of scattered particles in a fluid under the action of a uniform electric field [2,3]. It is a technique commonly used to separate charged molecules in today's cell biology laboratory. It can be used to separate proteins according to their size, shape, density and purity. It can also be used for plasmid analysis, which develops our understanding of bacteria becoming resistant to antibiotics. Regardless of the medium through which molecules are allowed to migrate, all electrophoretic separations depend upon the charge distribution of the molecules being separated. An electrical double layer is a structure that appears on the surface of a particle when it is embedded in a fluid. The particle might be a solid particle, a gas bubble, a fluid droplet or a porous body. It consists of two parallel layers of charge surrounding the particle. The first layer, the surface charge, contains ions adsorbed onto the particle. The second layer is composed of ions attracted to the surface charge, electrically screening the first layer. This second layer is almost associated with the particle. The electrophoretic mobility is defined as the ratio between the drift velocity of the scattered particle and the strength of the applied electric field. In this connection, a widely used equation in the theory of electrophoresis is Smoluchowski's equation [4]: $U = \epsilon\zeta E/(4\pi\eta)$, where U is the electrophoresis velocity of the particle, ζ is the zeta potential of the particle, E is the strength of the applied electric field, and ϵ and η are, respectively, the permittivity and the viscosity of the fluid dispersion medium. This equation works for scattered particles for any shape and any concentration and valid only for sufficiently thin double layer, when a particle of radius a is much greater than the Debye length, κ^{-1} : $a\kappa \gg 1$. This model is valid when the Debye length is only a few nanometres. In the literature, there are several studies in the electrophoretic theory at the steady state for the cases of thin and arbitrary electric double layer [5–8]. However, alternating electric fields have been used for

the measurements of electrophoretic phenomena in different situations. This motivated many researchers to study the effect of time-variant behaviour on electrophoretic and electroosmotic flows under various physical circumstances and different geometrical shapes [9–12]. The study of electrophoretic phenomena for the case of time-variant electric field is essential to interpret experimental observation and to improve and develop new separation devices.

The transient electrophoretic of a dielectric sphere was studied analytically by Morrison [13]. He utilized a thin double layer approximation and found that the particle attains its steady electroosmotic velocity at the instant as the electric field is suddenly imposed, showing that transient effect is remarkable for large particles. Ivory [10] recognized that the Morrison's assumptions, at short times, lead to unacceptable physical results that the viscous stresses in the fluid become unbounded at the outer surface of the double layer. In a trial to correct Morrison's solution, Ivory applied an interfacial boundary condition derived from the exact equations governing the fluid motion in the double layer. This condition is then used to investigate the dynamic response of the particle to a time-variant electric field. Keh and Huang [14] revisited the problem of transient electrophoresis of dielectric spheres and developed a successful model valid for arbitrary double layers and treated all the weakness of the previous papers dealing with this subject. In their paper, they studied analytically the dynamic electrophoretic response of a spherical dielectric particle suspended in a fluid to a step change in the applied electric field. The double layer enclosing the particle is considered either a small but finite thickness, or a very large thickness relative to the particle radius. Recently, Chen and Keh [15,16] employed the developmental model of [14] to investigate the transient response of electrolyte solution in the porous medium constructed by a homogeneous assemblage of parallel charged circular cylinders to the step application of an electric field and a pressure gradient in the axial and in the transverse directions, respectively, through the use of a unit cell model. More recently, the unit cell model was employed to investigate the transient electrophoresis of a suspension of dielectric spheres with constant zeta potential after the application of a step function electric field for the case of thin but finite double layer [17].

The subject of electrophoretic motion of charged particles embedded in a porous medium filled with an electrolyte solution is of particular interest in the area of chemical engineering and its related interdisciplinary fields such as environmental engineering [18–20] and biomedical engineering [21,22]. Few studies of this subject have been reported in the literature. In various practical applications, the electrophoresis in a porous medium is an effective separation technique. For instance, the separation of large bio-macromolecules in gel electrophoresis such as proteins and DNAs can be performed by moving samples through polymer gels under the action of an electric field [23,24]. However, electrophoresis through agarose or polyacrylamide gels is a standard method used to separate, identify and purify nucleic acids, since both these gels are porous in nature [25]. In addition to the above-cited classic applications, electrophoresis can be employed in the remediation treatment of contaminated soil in situ by applying an electric field through the wet soil to remove colloidal pollutants directly such as petroleum hydrocarbons [26,27]. Feng et al. [28] studied the motion of a chargeless sphere near planar confining boundaries in a fibre matrix modelled as a Brinkman medium. Tsai et al. [29] investigated theoretically the electrophoretic motion of a charged spherical particle in a porous medium by focusing on the boundary effect of a solid plane towards which the particle moves perpendicularly. This motivated us to consider in this article the time-dependent electrophoresis of a dielectric spherical particle embedded in a charged porous medium according to Brinkman's model and applying the transient model developed by Keh and Huang [14].

2. Field equations

The field equations governing an incompressible time-dependent viscous fluid flow through porous media, according to the Darcy–Brinkman model, are given [29,30], under the Stokesian assumption as:

$$\nabla \cdot \vec{q} = 0, \tag{2.1}$$

$$\frac{\rho}{\varphi}\frac{\partial \vec{q}}{\partial t} = \eta \nabla^2 \vec{q} - \frac{\eta}{K}\vec{q} - \nabla p + \frac{1}{\varphi}\vec{F}, \tag{2.2}$$

where $\vec{q}$ is the volume-averaged velocity vector, p is the pore average pressure, ρ and η are the density and the viscosity of the fluid, respectively, and (φ, K) represent the porosity and Darcy permeability of the porous medium. Here $\vec{F}$ represents the external body forces. The porous medium is characterized by its permeability which is a measure of the flow conductivity in the porous medium. It is also characterized by its porosity that is a ratio of the void space to the total volume of the medium. Note that the term $\vec{F}_D = \gamma \vec{q}$ in Brinkman's model represents an extra local friction force generated within the porous medium, where $\gamma = \eta/K$ is termed as friction coefficient. The permeability K is a scalar for isotropic porous medium; otherwise, K is a second-order tensor [31]. This model has two viscous terms: The first is the usual Darcy term and the second is analogous to the Laplacian term that appears in the Navier–Stokes equation. This equation is well accepted for porous media of high porosity. In most of the experimental methods used to predict a medium's permeability, investigators apply a constant pressure gradient to the porous medium in order to determine the average velocity of the flow from the measured fluid flow rate. Following this, the investigator applies Darcy's law to calculate the permeability coefficients [32,33]. Due to the complexity of the flow in the porous media, it is generally described in terms of macroscopic quantities. The macroscopic flow can be defined as the local volume average of the microscopic flow through the pores. Both the continuity and Brinkman equations are actually volume-averaged formulations. For media with low porosity, the Darcy law is a good approximation for the momentum equation, while Brinkman's model gives acceptable results for flows in high-porosity media. The validity of the Brinkman's model has been treated extensively in the literature [34–37].

3. Time-dependent electroosmotic flow through porous medium parallel to a dielectric plane

In this section, we consider the unsteady flow of an ionic fluid through a sparse of porous medium within an electric double layer abutting to a dielectric plane wall. As illustrated in Fig. 1, a uniform electric field E is suddenly applied tangentially to the wall at time t and maintained afterwards $t = 0$. The purpose of this section is to obtain the electroosmotic velocity at the outer edge of the double layer. This velocity will be used as a boundary condition for the mathematical modelling of the transient electrophoresis of dielectric spherical particle embedded in a sparse of porous medium [14–17]. The following assumptions are made: the gravitational forces are neglected and the uniformly distributed discrete charges over the plane wall are also neglected. Let a plane wall be at the coordinate surface, $y = 0$ and y-direction normal to the wall. We assume that the space charge density ρ_e and the electrostatic potential are function of y only, while the averaged velocity of the fluid q within the porous medium, which is in the direction of the applied electric field, is a function of (y, t). In this case, the equation of continuity for incompressible flow is satisfied automatically and the Brinkman equation reduces to

$$\frac{\rho}{\varphi}\frac{\partial q}{\partial t} = \eta \frac{\partial^2 q}{\partial y^2} - \frac{\eta}{K} q + \frac{\rho_e + \rho_f}{\varphi} E, \tag{3.1}$$

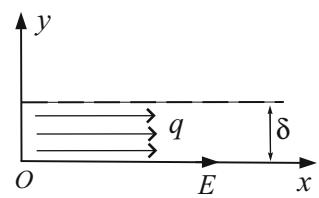

FIG. 1. Geometrical sketch of the double layer in porous medium

where ρ_f is the fixed charge density through the charged porous medium. Note that the last term in the modified Brinkman equation (3.1) represents the electrostatic effect due to the applied electric field [30]. Also note that the contributions from the pressure gradient and the electrostatic potential gradient cancel out in the Brinkman equation.

In connection with the above assumptions made, we assume also that the ionic diffusion time scale across the double layer is much shorter than the viscous time scale. This makes that the lateral potential distribution is not affected by the tangential applied electric field. Therefore, the Poisson equation [11] takes the form

$$\frac{\mathrm{d}^2\psi}{\mathrm{d}y^2} = -\frac{4\pi\,(\rho_e+\rho_f)}{\epsilon\,\varphi}, \tag{3.2}$$

where $\epsilon = 4\pi\epsilon_0\epsilon_r$, in which ϵ_r is the relative permittivity of the electrolyte solution and ϵ_0 is the permittivity of a vacuum. We assume that both ϵ and ρ_f are constant [38].

The governing equations (3.1) and (3.2) must be completed by the following initial and boundary conditions:

$$q = 0 \quad \text{at } t = 0, \tag{3.3}$$

$$\psi = \zeta,\ q = 0 \quad \text{at } y = 0, \tag{3.4}$$

$$\frac{\mathrm{d}\psi}{\mathrm{d}y} = 0,\ \frac{\partial q}{\partial y} = 0 \quad \text{at } y = \delta, \tag{3.5}$$

where ζ is the zeta potential at the surface of the wall and $y = \delta$ represents the equation of the outer edge of the electric double layer. Here δ will be considered as $\delta = b\,\kappa^{-1}$, where κ^{-1} is the Debye length (characteristic thickness of the double layer) and b is a positive number which is for clear fluid ($K \to \infty$) in the range between 3 and 5 [14].

It should be noted that the thin double layer approximation is accurate when

$$(\kappa\,a)^{-1}\cosh(Ze\zeta/2\sigma T_c) \ll 1, \tag{3.6}$$

where Z is the charge number of the electrolyte, assumed the same for both ions, e is the charge of one proton, T_c is the absolute temperature, and σ is Boltzmann's constant [39].

3.1. Steady-state solution

To find the starting solution of the initial boundary value problem (3.1)–(3.5), we first have to define and solve the steady-state problem:

$$\lim_{t\to\infty}\frac{\partial q}{\partial t} = 0, \quad \text{and} \quad \lim_{t\to\infty} q(y,t) = q_s(y). \tag{3.7}$$

Then the differential equation satisfied by the steady-state solution $q_s(y)$ is

$$\frac{\mathrm{d}^2 q_s}{\mathrm{d}y^2} - \frac{1}{K}\,q_s + \frac{\rho_e+\rho_f}{\eta\,\varphi}\,E = 0. \tag{3.8}$$

Eliminating the total charge densities term $(\rho_e+\rho_f)$ between Eqs. (3.2) and (3.8), we get the differential equation satisfied by q_s:

$$\left(\frac{\mathrm{d}^2}{\mathrm{d}y^2} - \alpha^2\right) q_s = \frac{\epsilon\,E}{4\pi}\,\frac{\mathrm{d}^2\psi}{\mathrm{d}y^2}, \tag{3.9}$$

where $\alpha = 1/K^{1/2}$ is the dimensional permeability parameter. Using boundary conditions (3.4) and (3.5), it is found that the steady-state limiting solution is given by the expression

$$q_s = -\frac{\epsilon E}{4\pi\eta}\Big[\zeta\frac{\cosh\alpha(y-\delta)}{\cosh\alpha\delta} - \psi(y) + \alpha\int_0^\delta \psi(\xi)\frac{\sinh\alpha y\,\cosh\alpha(\delta-\xi)}{\cosh\alpha\delta}\,\mathrm{d}\xi - \alpha\int_0^y \psi(\xi)\,\sinh\alpha(y-\xi)\,\mathrm{d}\xi\Big]. \tag{3.10}$$

3.2. Time-dependent solution

To find the fluid velocity profile $q(y,t)$ along the plane wall, let

$$q_\tau(y,t) = q(y,t) - q_s(y). \tag{3.11}$$

Inserting Eq. (3.11) into Eqs. (3.1)–(3.5) and using the differential equation (3.9), we get the initial boundary value problem satisfied by $q_\tau(y,t)$:

$$\frac{1}{\nu}\frac{\partial q_\tau}{\partial t} + \alpha^2 q_\tau = \frac{\partial^2 q_\tau}{\partial y^2}, \tag{3.12}$$

and

$$q_\tau = -q_s(y) \quad \text{at } t = 0, \tag{3.13}$$

$$q_\tau = 0 \quad \text{at } y = 0, \tag{3.14}$$

$$\frac{\partial q_\tau}{\partial y} = 0 \quad \text{at } y = \delta, \tag{3.15}$$

where $\nu = \eta\varphi/\rho$ is the effective kinematic viscosity. Using the separation of variables techniques, we obtain the solution of q_τ as

$$q_\tau(y,t) = -\sum_{n=1}^{\infty}\left(2\delta^{-1}\int_0^\delta q_s(y)\sin(\lambda_n y)\,\mathrm{d}y\right)\sin(\lambda_n y)\,e^{-(\lambda_n^2+\alpha^2)\nu t}, \tag{3.16}$$

where $\lambda_n = (2n-1)\pi/(2\delta)$. Substituting (3.10) and (3.16) into (3.11) gives the fluid averaged velocity distribution $q(y,t)$ along the plane wall. The series term in the averaged velocity $q(y,t)$ converges rapidly for large time parameter $\nu\,t/\delta^2$. The averaged fluid velocity $U_\delta(t)$ at large distance from the surface of the plane wall (with $\kappa y \geq \kappa\delta = b$) can be obtained as

$$U_\delta = -\frac{\epsilon\zeta E}{4\pi\eta}\left(\frac{1}{\cosh\alpha\delta} + \sum_{n=1}^{\infty}\frac{2(-1)^n\lambda_n}{\delta\,(\alpha^2+\lambda_n^2)}\,e^{-(\lambda_n^2+\alpha^2)\nu t}\right), \tag{3.17}$$

where $\psi(y) \to 0$ far from the plane wall. Taking δ as the half-thickness of a capillary slit filled with a sparse of the porous medium, Eqs. (3.16) and (3.17) can also represent the corresponding electroosmotic averaged velocity of the fluid within the slit [11].

4. Time-dependent electrophoresis of a spherical particle embedded in a porous medium with a thin double layer

Consider the unsteady electrophoretic motion of a dielectric spherical particle of radius a. The particle is placed in an electrolyte-saturated porous medium of permeability K, which can be determined either by theoretical prediction or by experimental measurement. When the Brinkman equation is scaled by the particle radius a and made dimensionless, a parameter, $\alpha' = a/K^{1/2}$, appears. Therefore, α' describes the ratio of the particle dimension to the fibre interaction layer thickness, $K^{1/2}$; that is K depends on the fibre spacing f_s and to a lesser extent on the fibre radius f_r [28]. A spherical particle of radius a will

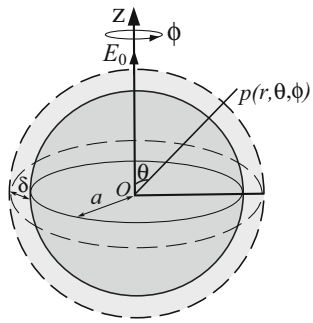

FIG. 2. Geometrical sketch for the electrophoresis of a sphere in porous medium

not be able to translate in a rigid periodic fibre array when the open spacing between fibres, f_s, is less than the sphere diameter. Thus for a rigid fibre array, the Brinkman parameter $\alpha' = a/K^{1/2}$ describing the motion of a spherical particle in a Brinkman medium will have a maximum value if the particle is not to be trapped by the fibres. For a periodic fibre array one must satisfy an assumption on K that is $f_s > 2a$ [28]. Feng et al. [28] show that, for a spherical particle diffusing in a rigid fibre array, the maximum value of α' is approximately 1.5 and varies weakly with the fibre radius. This restriction on α' will not apply if a large particle is forced to move through a highly flexible matrix with weak fibre adhesion energy. Tsay and Weinbaum [40] indicated that $K^{1/2}$ is of the same order as the fibre spacing f_s. The main point in using the Brinkman equation to evaluate the drag force exerted on a diffusing particle is the constraint on α' for which the effective medium theory applies. The parameter α' describes the transition from small-scale viscous motion given by the Stokes equation to larger-scale pressure-driven motions ruled by Darcy's equation. We use a spherical coordinate system (r, θ, ϕ) with the origin at the centre of the particle. Further, the particle enveloped by a finite thin electric double layer ($\kappa a \gg 1$) in an electrolyte fluid-saturated porous medium. Initially, $t = 0$ a constant electric field E_0 is imposed suddenly throughout the system in the $\theta = 0$ direction and maintained afterwards, as shown in Fig. 2. As a result, the particle experiences an electrophoretic motion with a time-dependent velocity in the same direction as E_0. Note that $U(t)$ is unknown and has to be determined with $U(0) = 0$. The Reynolds number of this electrokinetic flow is very low; therefore, the motion of the electrolyte solution-saturated porous medium outside the double layer can be modelled by the unsteady Brinkman equation (2.2). Since the charge density, outside the double layer, approaches zero as $e^{-\kappa y}$, the outer region is electrically neutral [39]. In the electrolyte, cations and anions are dissolved and the amount of each ion species is the same because of the charge neutrality of the system [41]. Also the electrolyte outside the double layer is of constant conductivity and of uniform composition. Due to the symmetry of the problem we have $\partial/\partial\phi = 0$. It is convenient to use the stream function $\Psi(r, \theta)$ which is related to the velocity components $q_r(r, \theta)$, $q_\theta(r, \theta)$ by

$$q_r = -\frac{1}{r^2 \sin\theta}\frac{\partial \Psi}{\partial \theta}, \qquad q_\theta = \frac{1}{r \sin\theta}\frac{\partial \Psi}{\partial r}. \tag{4.1}$$

Therefore, the stream function satisfied by the fourth-order differential equation:

$$L_{-1}\left(L_{-1} - \alpha^2 - \frac{1}{\nu}\frac{\partial}{\partial t}\right)\Psi = 0, \tag{4.2}$$

where L_{-1} is the axisymmetric Stokesian operator:

$$L_{-1} = \frac{\partial^2}{\partial r^2} + \frac{\sin\theta}{r^2}\frac{\partial}{\partial \theta}\left(\frac{1}{\sin\theta}\frac{\partial}{\partial \theta}\right). \tag{4.3}$$

Solving the Laplace equation, $\nabla^2 V = 0$ governing the electric potential V in the medium outside the thin double layer surrounding the dialectic spherical particle and applying the non-conducting (zero-flux) condition at the outer edge of the double layer, $\partial V/\partial r = 0$ at $r = a^+$ as well as the condition: $(V + E_0 r\cos\theta)$ is finite in $r > a$. The solution of this problem is $V = -E_0[r + a^3/(2r^2)]\cos\theta$. Therefore, the local tangential electric field E_θ in θ-direction at the surface of the dielectric sphere caused by the imposed electric field is

$$E_\theta = -\frac{1}{r}\frac{\partial V}{\partial \theta}\Big|_{r=a^+} = -\frac{3}{2}E_0 \sin\theta. \tag{4.4}$$

This tangential electric field interacts with the thin double layer to produce a local electroosmotic velocity at $r = a^+$. Thus, the initial and boundary conditions for the velocity components q_r and q_θ of the fluid through the porous medium can be expressed as:

$$t = 0: \quad q_r = q_\theta = 0, \tag{4.5}$$

$$r = a^+: \quad q_r = U\cos\theta, \tag{4.6}$$

$$q_\theta = -U\sin\theta + \frac{3\epsilon\zeta E_0}{8\pi\,\eta}\Big(\frac{1}{\cosh\alpha\delta} + \sum_{n=1}^{\infty}\frac{2(-1)^n\lambda_n}{\delta(\alpha^2+\lambda_n^2)}e^{-(\lambda_n^2+\alpha^2)\nu t}\Big)\sin\theta, \tag{4.7}$$

$$r \to \infty: \quad q_r = q_\theta = 0, \tag{4.8}$$

where $r = a^+$ represents the outer edge of the thin double layer. The unknown velocity $U(t)$ of the dielectric particle can be written as

$$U(t) = U_0\,\mu(t), \tag{4.9}$$

where $U_0 = \lim_{t\to\infty} U(t)$ is the steady-state particle's velocity, which is given by the modified Smoluchowski equation for porous medium [4],

$$U_0 \equiv \frac{\epsilon\zeta E_0}{4\pi\,\eta\cosh\alpha\delta}. \tag{4.10}$$

Note that $\mu(0) = 0$ and $\lim_{t\to\infty}\mu(t) = 1$.

The starting hydrodynamic drag force (in the z-direction) exerted by the porous fluid on the spherical boundary surface can be determined from [14,42]

$$F(t) = \pi\,\eta\,a\int_0^\pi \Big[r^4\sin^3\theta\,\frac{\partial}{\partial r}\Big(\frac{L_{-1}\Psi}{r^2\sin^2\theta}\Big) - \alpha^2 r^2\sin\theta\,\frac{\partial\Psi}{\partial r} - \frac{1}{\nu}\,r^3\sin^2\theta\,\frac{\partial q_\theta}{\partial t}\Big]_{r=1^+}\mathrm{d}\theta, \tag{4.11}$$

where, here and in all subsequent expressions and parameters, we normalized all lengths with respect to the radius of the particle a.

This drag force, $F(t)$, is equal to the rate of change of the electrophoretic particle momentum, i.e.

$$F(t) = M\,\frac{\mathrm{d}U}{\mathrm{d}t}, \tag{4.12}$$

where M is the mass of the particle.

The velocity at the surface of the dielectric particle $r = 1^+$ caused by the electroosmotic effect, which drives the electrophoretic motion of the particle, is called the apparent velocity slip and is given by the last term of Eq. (4.7). A normalized quantity of this time-dependent velocity slip can be expressed as

$$V_{\mathrm{slip}} = \frac{1}{\cosh\alpha\delta} + \sum_{n=1}^{\infty}\frac{2(-1)^n\lambda_n}{\delta(\alpha^2+\lambda_n^2)}e^{-(\lambda_n^2+\alpha^2)\nu t}, \tag{4.13}$$

which is a function of the parameter $\nu t/\delta^2[= (\kappa a/b)^2(\nu t/a^2)]$ and the non-dimensional permeability parameter $\alpha = a/K^{1/2}$.

4.1. Solution in the Laplace transform domain

Introducing the Laplace transform (denoted by an overbar) defined by the formula

$$\bar{f}(r,\theta;s) = \int_0^\infty f(r,\theta;t)\, e^{-st}\, \mathrm{d}t, \tag{4.14}$$

into Eq. (4.2) and using the initial condition (4.5), we obtain

$$L_{-1}(L_{-1} - \beta^2)\bar{\Psi} = 0, \tag{4.15}$$

and the transformed boundary conditions are

$$r = 1^+ : \quad \bar{q}_r = \bar{U}\cos\theta, \tag{4.16}$$

$$\bar{q}_\theta = -\bar{U}\sin\theta + \frac{3\epsilon\zeta E_0}{8\pi\,\eta}\left(\frac{1}{s\cosh\alpha\delta} + \sum_{n=1}^{\infty}\frac{2(-1)^n a^2\lambda_n}{\delta(\alpha^2+\lambda_n^2)\,(\alpha^2\nu+\lambda_n^2\nu+a^2 s)}\right)\sin\theta, \tag{4.17}$$

$$r \to \infty : \quad \bar{q}_r = \bar{q}_\theta = 0, \tag{4.18}$$

where $\beta = \sqrt{\alpha^2 + a^2 s/\nu}$.

The bounded solution of (4.15) is given by

$$\bar{\Psi} = \left(\frac{A}{r} + \frac{B}{r}\,(\beta\, r + 1)\, e^{-\beta\, r}\right)\sin^2\theta, \tag{4.19}$$

where the two unknown coefficients A and B are functions of the transform parameter s and determined using the boundary conditions (4.16) and (4.17), with the result

$$A = \frac{U_0}{2\beta^2}\big(3(\beta+1)\,\vartheta\cosh\alpha\delta - (\beta^2+3\beta+3)\,\bar{\mu}(s)\big), \tag{4.20}$$

$$B = \frac{3U_0}{2\beta^2}(\bar{\mu}(s) - \vartheta\cosh\alpha\delta)e^{\beta}, \tag{4.21}$$

with

$$\vartheta = \frac{1}{s\cosh\alpha\delta} + \sum_{n=1}^{\infty}\frac{2(-1)^n a^2\lambda_n}{\delta\,(\alpha^2+\lambda_n^2)\,(\alpha^2\,\nu+\nu\,\lambda_n^2+a^2 s)}.$$

Therefore, the Laplace transform of the drag force, given by Eq. (4.11), acting on the spherical particle will be

$$\bar{F}(s) = \pi\,\eta\,a\int_0^\pi\left[r^4\sin^3\theta\,\frac{\partial}{\partial r}\left(\frac{L_{-1}\bar{\Psi}}{r^2\sin^2\theta}\right) - \alpha^2 r^2\sin\theta\,\frac{\partial\bar{\Psi}}{\partial r} - \frac{s}{\nu}\,r^2\sin\theta\,\frac{\partial\bar{\Psi}}{\partial r}\right]_{r=1^+}\mathrm{d}\theta, \tag{4.22}$$

$$= \frac{4}{3}\pi\,\eta\,a\beta^2\big(A - 2B\,(\beta+1)\,e^{-\beta}\big). \tag{4.23}$$

Therefore, we obtain the transformed drag force as

$$\bar{F}(s) = 6\pi\,aU_0\eta\left[(\beta+1)\,\vartheta\,\cosh\alpha\delta - \left(\frac{\beta^2}{9}+\beta+1\right)\bar{\mu}(s)\right]. \tag{4.24}$$

Taking the Laplace of Eq. (4.12) and noting that $U(0) = 0$, we obtain

$$\bar{F}(s) = Ms\,U_0\bar{\mu}(s), \tag{4.25}$$

where

$$\bar{\mu}(s) = \frac{\sqrt{\alpha^2+a^2 s/\nu}+1}{\alpha^2/9+\sqrt{\alpha^2+a^2 s/\nu}+1+\chi^{-2}a^2 s/\nu}\left(\frac{1}{s}+\sum_{n=1}^{\infty}\frac{2(-1)^n\lambda_n a^2\cosh\alpha\delta}{\delta\,(\alpha^2+\lambda_n^2)\,(\alpha^2\nu+\lambda_n^2\nu+a^2 s)}\right), \tag{4.26}$$

in which $\chi^2 = 9m/(2M+m)$ and $m = (4/3)\pi a^3\rho/\varphi$. Clearly, $0 \le \chi \le 3$, with the upper and lower bounds occurring at the limits $M/m = 0$ and $M/m \to \infty$, respectively. Note that the spherical particle velocity vanishes as $M/m \to \infty$, while it has a large value at $M/m = 0$.

It is convenient to define a non-dimensional time T and its counterpart S in the Laplace transform as [14]

$$T = \frac{t\,\nu\,\chi^2}{a^2}, \quad \text{and} \quad S = \frac{a^2 s}{\nu\,\chi^2}. \tag{4.27}$$

In terms of these new variables (T, S), we obtain

$$\begin{aligned}\bar{\mu}^*(s) = {} & \frac{9\big(\sqrt{S\chi^2+\alpha^2}-\chi^2+1\big)S+\alpha^2\sqrt{S\chi^2+\alpha^2}+9-8\alpha^2}{9(S-\ell)\,(S-\jmath)} \\ & \times\left(\frac{1}{S}+\sum_{n=1}^{\infty}\frac{2(-1)^n\chi\sqrt{\omega_n}\cosh\alpha\delta}{\delta\,(\alpha^2+\chi^2\omega_n)\,(\alpha^2/\chi^2+\omega_n+S)}\right),\end{aligned} \tag{4.28}$$

where

$$\bar{\mu}^*(s) = \bar{\mu}(s)\nu\chi^2/a^2,\ \sqrt{\omega_n} = (2n-1)\pi a/(2\chi\delta) = (2n-1)\pi\kappa a/(2\chi b),$$

while ℓ and $\jmath$ are the roots of the quadratic equation:

$$S^2+\left(\frac{2\alpha^2}{9}-\chi^2+2\right)S+\frac{(\alpha^2+9)^2}{81}-\alpha^2 = 0. \tag{4.29}$$

4.2. Inverse of the Laplace transforms

The electrophoretic mobility can be obtained by the inverse Laplace transform of Eq. (4.28). After algebraic manipulation, we obtain

$$\begin{aligned}\mu = {} & \frac{e^{\ell T}}{9(\ell-\jmath)\ell}\Big(\chi\sqrt{\Lambda^2+\ell}\,(\Lambda^2\chi^2+9\ell)\,\mathrm{erf}\big(\sqrt{T(\Lambda^2+\ell)}\big)-(8\Lambda^2\chi^2+9\ell\chi^2-9\ell-9)\Big) \\ & -\frac{e^{\jmath T}}{9(\ell-\jmath)\jmath}\Big(\chi\sqrt{\Lambda^2+\jmath}\,(\Lambda^2\chi^2+9\jmath)\,\mathrm{erf}\big(\sqrt{T(\Lambda^2+\jmath)}\big)-(8\Lambda^2\chi^2+9\jmath\chi^2-9\jmath-9)\Big) \\ & +\frac{1}{9\ell\jmath}\big(\Lambda^3\chi^3\,\mathrm{erf}\big(\Lambda\sqrt{T}\big)-(8\Lambda^2\chi^2-9)\big)+\sum_{n=1}^{\infty}\frac{2(-1)^n\lambda_n\cosh\alpha\delta}{\delta\,(\alpha^2+\lambda_n^2)}\left[\frac{e^{\ell T}}{9(\ell-\jmath)\,(\Lambda^2+\ell+\omega_n)}\right. \\ & \times\Big(\chi\sqrt{\Lambda^2+\ell}\,(\Lambda^2\chi^2+9\ell)\,\mathrm{erf}\big(\sqrt{T(\Lambda^2+\ell)}\big)-(8\Lambda^2\chi^2+9\ell\chi^2-9\ell-9)\Big) \\ & -\frac{e^{\jmath T}}{9(\ell-\jmath)(\Lambda^2+\jmath+\omega_n)}\Big(\chi\sqrt{\Lambda^2+\jmath}\,(\Lambda^2\chi^2+9\jmath)\,\mathrm{erf}\big(\sqrt{T(\Lambda^2+\jmath)}\big)-(8\Lambda^2\chi^2+9\jmath\chi^2-9\jmath-9)\Big) \\ & \left.-\frac{e^{-(\Lambda^2+\omega_n)T}}{9(\Lambda^2+\ell+\omega_n)(\Lambda^2+\jmath+\omega_n)}\Big((\sqrt{\omega_n}\,\chi-1)(\Lambda^2\chi^2-9\Lambda^2-9\omega_n)\,\mathrm{erfi}\big(\sqrt{\omega_n T}\big)-9\omega_n\chi^2-9\Big)\right],\end{aligned} \tag{4.30}$$

where $\Lambda = \alpha/\chi$, while $\mathrm{erf}(x)$ and $\mathrm{erfi}(x)$ represent the error function and imaginary error function, respectively.

Equation (4.30) indicates that the non-dimensional start-up of electrophoretic mobility μ is a function of the following parameter:

(1) The non-dimensional time T.
(2) The permeability parameter α of the porous medium.

(3) The Debye length (inverse double layer thickness) parameter $\kappa a/b\,(=a/\delta)$.
(4) The mass density parameter $\chi\,(0\le\chi\le 3)$.

The infinite series in Eq. (4.30) is the contribution from the dynamic response of the electroosmotic porous flow at the particle surface after the electric field is suddenly applied. In the limit $\alpha=0$, the normalized electrophoretic mobility μ reduce to the results obtained by Keh and Huang [14].

5. Time-dependent translation of a spherical particle caused by a suddenly applied body force

Initially at the time $t=0$, a constant force F_A is applied on the particle in the $\theta=0$ direction and kept acting on the particle afterwards. When the Reynolds number is low, the stream function of the fluid flow through the porous medium is governed by Eq. (4.2). The initial and boundary conditions of this problem are still given by Eqs. (4.5)–(4.8), but with Eq. (4.7) replaced by

$$r=1: \quad q_\theta=-U\sin\theta, \tag{5.1}$$

where $U(t)$ is the unsteady translational velocity of the particle to be determined, which can be expressed according to Brinkman model as $U=U_0\mu(t)$ with [28]

$$U_0\equiv\frac{F_A}{6\pi\,\eta\,a(\alpha^2/9+\alpha+1)}, \tag{5.2}$$

where also $\mu(0)=0$ and $\lim_{t\to\infty}\mu(t)=1$.

Again the transformed differential equations and the transformed boundary conditions are still the same as the previous section except (4.17) is replaced by

$$r=1: \quad \bar{q}_\theta=-\bar{U}\sin\theta. \tag{5.3}$$

Therefore, the stream function is still given by (4.19) where A and B are now replaced by

$$A=-\frac{U_0}{2\beta^2}\,(\beta^2+3\beta+3)\,\bar{\mu}(s), \tag{5.4}$$

$$B=\frac{3U_0}{2\beta^2}\,\bar{\mu}(s)e^{\beta}. \tag{5.5}$$

The time-dependent drag force F acting on the spherical boundary $r=1$ by the fluid through the porous medium can also be determined from Eq. (4.11). Therefore, the momentum equation of the particle takes the form

$$F_A+F=M\,\frac{\mathrm{d}U}{\mathrm{d}t}. \tag{5.6}$$

Taking the Laplace transform of Eq. (5.6) and using Eqs. (4.23), (5.4) and (5.5), one obtains

$$\bar{\mu}(s)=\frac{1}{s}\left(\frac{\alpha^2}{9}+\alpha+1\right)\left(\frac{\alpha^2}{9}+\sqrt{\alpha^2+\frac{a^2s}{\nu}}+1+\frac{a^2s}{\nu\,\chi^2}\right)^{-1}. \tag{5.7}$$

Again, in terms of the non-dimensional variables defined by (4.26) and $\bar{\mu}^*(s)=\bar{\mu}(s)\nu\chi^2/a^2$, Eq. (5.7) becomes

$$\bar{\mu}^*(s)=\left(\frac{\alpha^2}{9}+\alpha+1\right)\frac{\alpha^2/9-\sqrt{S\chi^2+\alpha^2}+S+1}{S(S-\ell)\,(S-\jmath)}, \tag{5.8}$$

where ℓ and $\jmath$ are the roots of Eq. (4.29). The inverse Laplace transform of Eq. (5.8) leads to

$$\mu = \frac{\alpha^2/9+\alpha+1}{9}\left[\frac{e^{\ell T}}{(\ell-\jmath)\ell}\left(\Lambda^2\chi^2 - 9\chi\sqrt{\Lambda^2+\ell}\,\mathrm{erf}\big(\sqrt{T(\Lambda^2+\ell)}\big)+9\ell+9\right)\right.$$
$$\left. - \frac{e^{\jmath T}}{(\ell-\jmath)\jmath}\Big(9+9\jmath+\Lambda^2\chi^2-9\chi\sqrt{\Lambda^2+\jmath}\,\mathrm{erf}\big(\sqrt{T(\Lambda^2+\jmath)}\big)\Big)+\frac{1}{\ell\jmath}\big(\Lambda^2\chi^2-9\Lambda\chi\,\mathrm{erf}\big(\Lambda\sqrt{T}\big)+9\big)\right]. \tag{5.9}$$

For $\alpha = 0$, we get the same result for the normalized electrophoretic mobility μ as obtained by Keh and Huang [14].

6. Time-dependent electrophoresis of a dielectric spherical particle with a thick double layer

In this section, we use the results of the previous section to investigate the unsteady electrophoresis problem of a small dielectric spherical particle enclosed by a thick double layer ($\kappa a \to 0$) in an electrolyte solution through a porous medium. At the time $t = 0$, a constant electric field E_0 is imposed in the $\theta = 0$ direction and maintained afterwards. Due to the fact that the gradient of the electrostatic potential is a small quantity of order $\kappa|\zeta|$, the effect of electric force in the Brinkman equation of motion is ignored. Thus, in the limit of low Reynolds number, the flow field enclosed by the electrophoretic particle is also governed by Eqs. (4.2), (4.5), (4.6), (4.8) and (5.1).

Using the Debye–Hückel approximation [43], the total surface charge Q on a dielectric spherical particle of radius a is given by

$$Q = a\,\epsilon\,\zeta. \tag{6.1}$$

The body force acting on the dielectric particle, due to the electric field, is

$$F_A = QE_0 = a\,\epsilon\,\zeta\,E_0. \tag{6.2}$$

Therefore, expression (6.2) indicates that the unsteady motion of a particle under the effect of step function electric field is the same as that treated in Sec. 5 for the starting translation of a spherical particle caused by a suddenly applied body force with the steady particle velocity U_0, in Eq. (5.2), replaced by

$$U_0 \equiv \frac{\epsilon\zeta\,E_0}{6\pi\,\eta(\alpha^2/9+\alpha+1)}. \tag{6.3}$$

7. Results and discussion

7.1. Velocity slip results

In this subsection, we present the results of the apparent velocity slip, given by (4.13), at the outer boundary of the double layer caused by the electroosmotic effect. Figure 3 indicates the plots of V_{slip} for various values of the dimensionless elapsed time $\nu t/a^2$, the permeability parameter α and $\kappa a/b$. When a colloidal particle is suspended in a viscous fluid with kinematic viscosity ν of order 10^{-6} m^2/s and has a radius of order $1\,\mu\mathrm{m}$ for the case of thin double layer and $0.1\mu\mathrm{m}$ for the case of thick double layer, these relaxation responses correspond to times of order μs [14]. For a fixed value of α or $\kappa a/b$, the apparent velocity slip at the particle surface increases monotonically and quickly with the time from zero at $t = 0$ to its steady-state magnitude as $t \to \infty$. Again for fixed values of α and $\nu t/a^2$, the normalized velocity slip decreases monotonically with a decrease in $\kappa a/b$ or an increase in the thickness of the double layer. Due to the fact that the response time of the fluid within an infinitely thin double layer to the applied

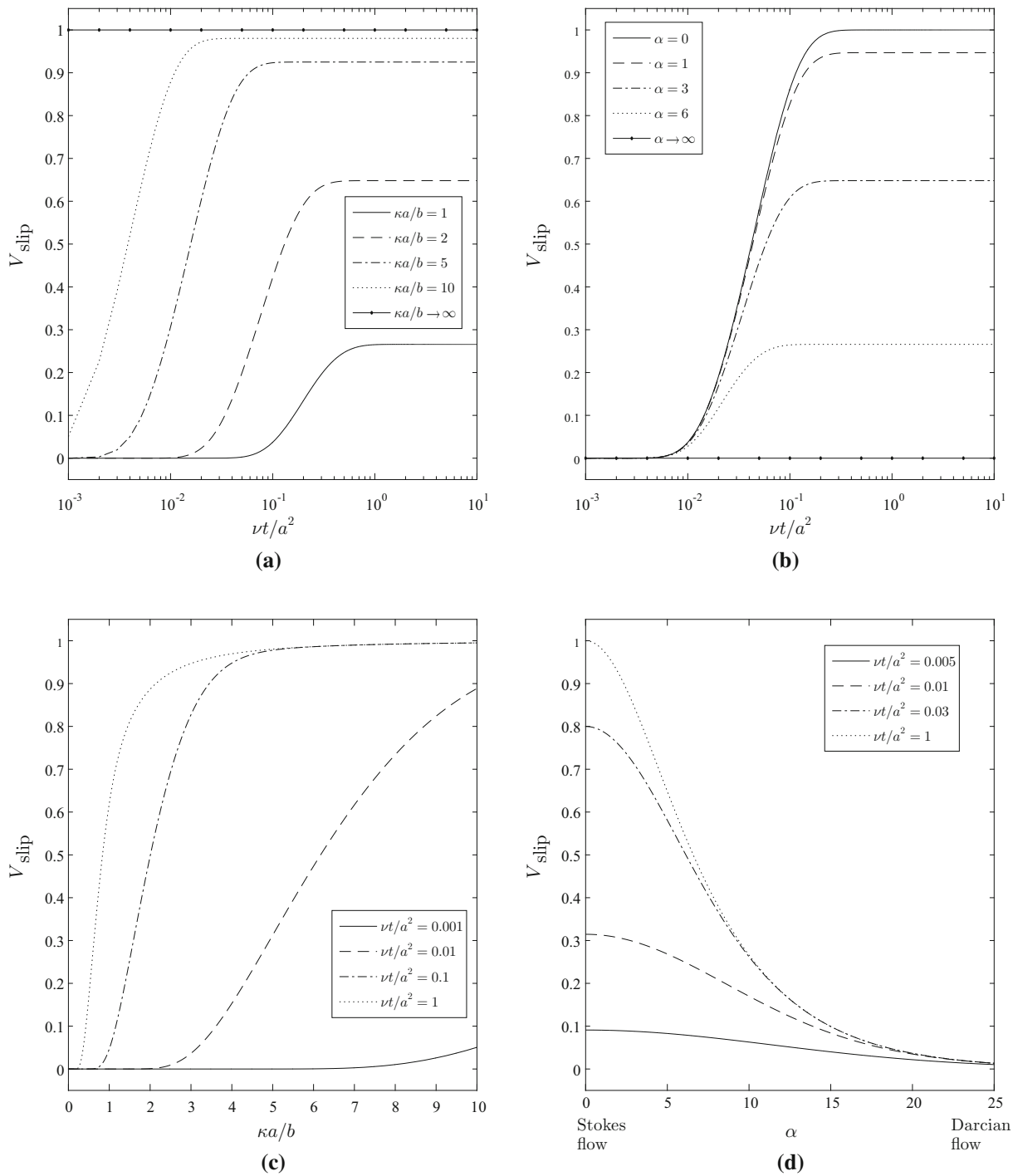

FIG. 3. Variation of the normalized velocity slip V_{slip} at the particle surface. Calculations of V_{slip} in **a**, **b** versus the non-dimensional elapsed time $\nu t/a^2$ at $\alpha = 2$ and $\kappa a/b = 3$, respectively, **c** versus the parameter $\kappa a/b$ at $\alpha = 2$, and **d** versus the permeability parameter α with $\kappa a/b = 5$

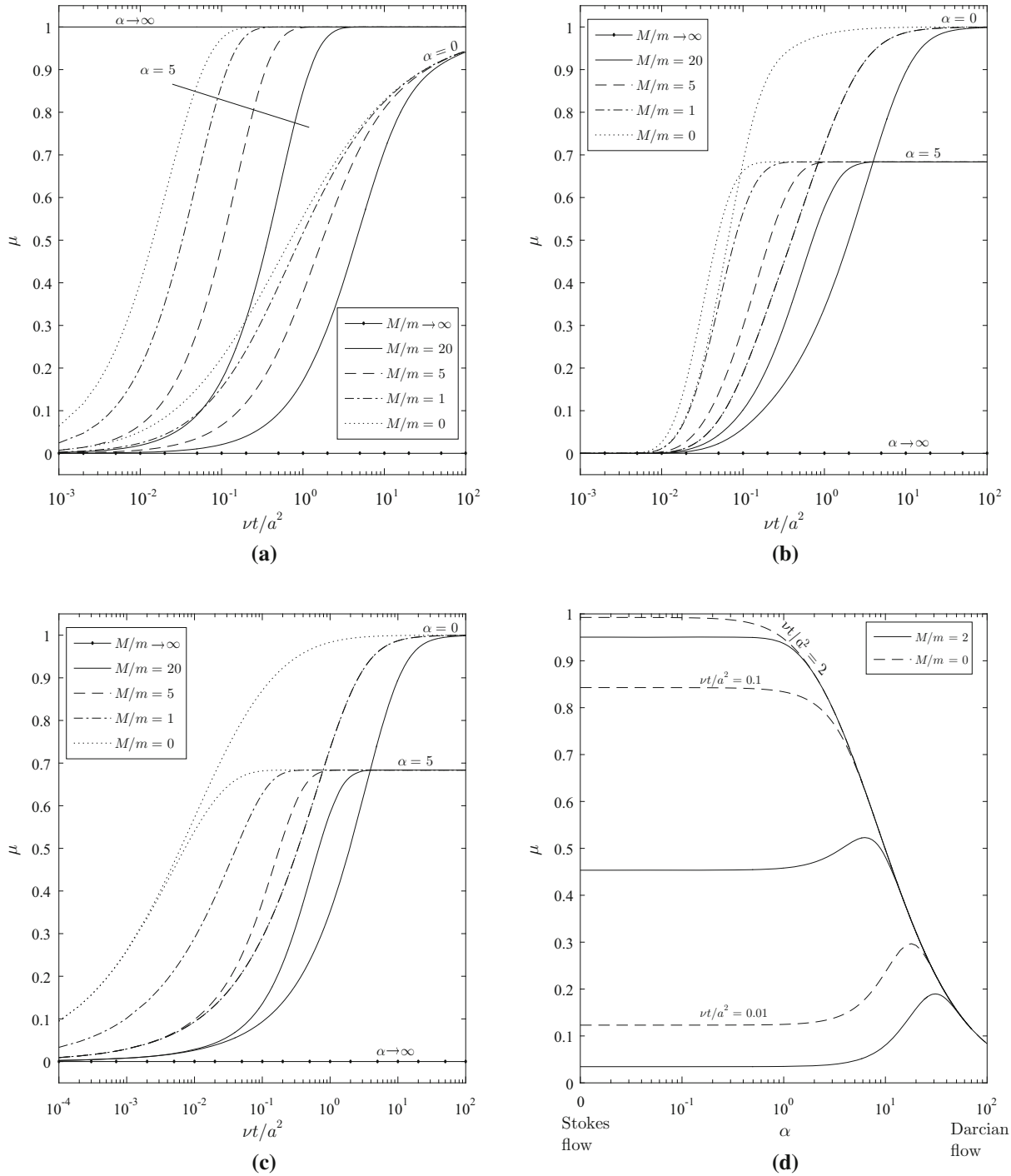

FIG. 4. Variation of the normalized electrophoretic mobility μ versus the non-dimensional elapsed time $\nu t/a^2$ with M/m and α as parameters. Calculations of **a** $\kappa a/b = 0$, **b** $\kappa a/b = 3$, **c** $\kappa a/b \to \infty$, and calculations of μ in **d** versus the permeability parameter α with $\kappa a/b = 5$

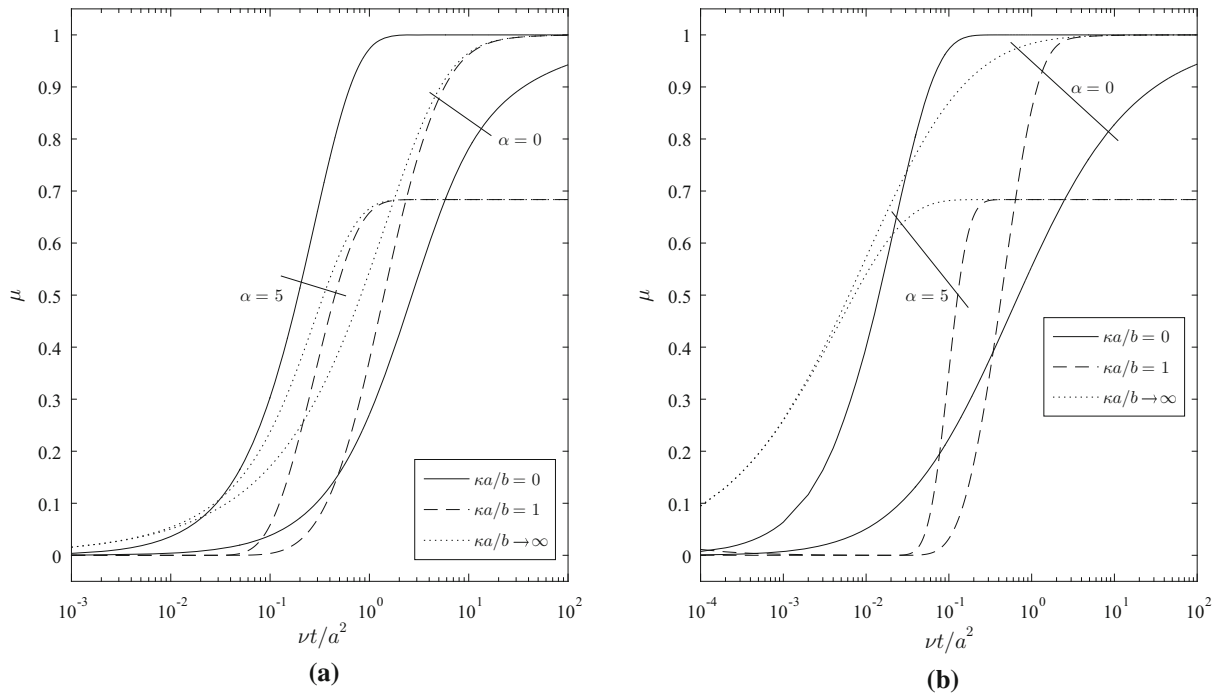

FIG. 5. Variation of the normalized electrophoretic mobility μ versus the non-dimensional elapsed time $\nu t/a^2$ with $\kappa a/b$ and α as the parameters. Calculations of **a** $M/m = 10$ and **b** $M/m = 0$

electric field is zero, $V_{\text{slip}} = 1$ as $\kappa a/b \to \infty$, regardless of the duration and for any finite value of the permeability parameter. For the entire range of the permeability parameter under the thin double layer assumption $\kappa a/b \gg 1$, the velocity slip approaches its steady-state quantity rapidly, indicating that it is justified to neglect the relaxation effect of this velocity slip in Morrison [13] analysis. For any specified value of the permeability parameter, the time-dependent duration of V_{slip} to approach its steady state is shorter for thin double layer and longer as the thickness of the double layer increases. Again for a fixed value of $\kappa a/b$, the time-dependent duration of V_{slip} to approach its steady state is shorter for low permeability and is longer for high permeability and reaches a maximum duration for the Stokes clear fluids. It should be noted here that the results for the case of the clear fluids $\alpha = 0$ ($K \to \infty$) are in perfect agreement as that of Keh and Huang [14]. We note that, for any fixed value of dimensionless time $\nu t/a^2$, the velocity slip decreases monotonically with an increase in the permeability parameter α. It indicates that the velocity slip has maximum relative effects on the flow when the particle surface was surrounded by Stokes' flow ($\alpha = 0$). For fixed values of α and $\kappa a/b$, V_{slip} increases with the increase in dimensionless elapsed time. For any value of $\nu t/a^2$ and as α tends to the Darcian limit, $V_{\text{slip}} \to 0$.

7.2. Electrophoretic mobility results

The expressions for the starting electrophoretic mobility $\mu(t)$ of a dielectric spherical particle embedded in a porous medium due to the application of a step function electric field are given by (4.30) and (5.9) for the cases of thin ($\kappa a/b \gg 1$) and thick ($\kappa a/b \to 0$) double layers, respectively. Note that expressions (4.30) and (5.9) are normalized with respect to their corresponding steady state. The electrophoretic mobilities are functions of the dimensionless elapsed time, the mass ratio M/m and the permeability

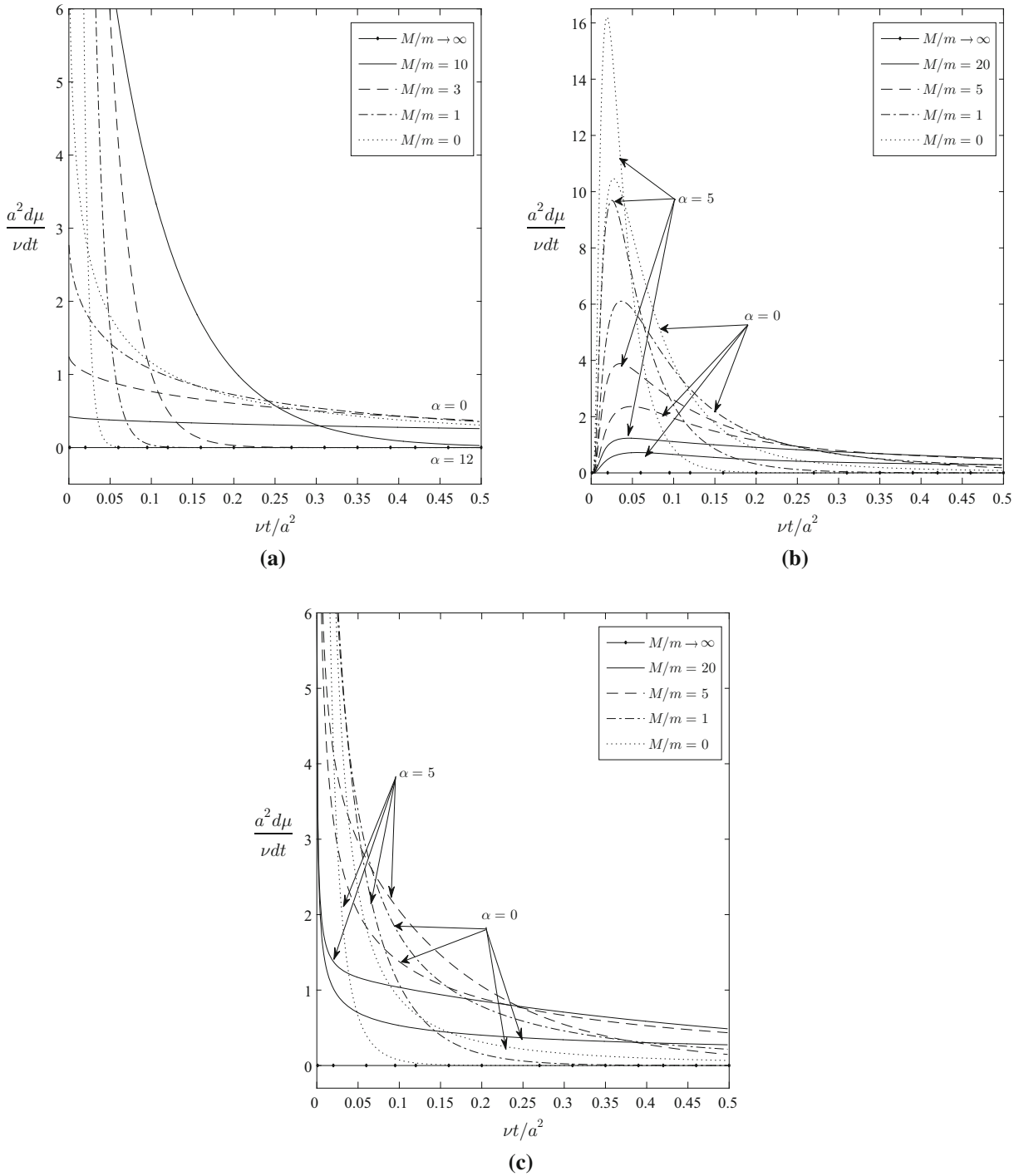

FIG. 6. Variation of the normalized electrophoretic acceleration $(a^2/\nu)d\mu/dt$ versus the non-dimensional elapsed time $\nu t/a^2$ with M/m and α as the parameters. Calculations of **a** $\kappa a/b = 0$, **b** $\kappa a/b = 3$ and **c** $\kappa a/b \to \infty$

parameter. Figure 4a–c shows plots of $\mu(t)$ against $\nu t/a^2$ for the cases (a) $\kappa a/b = 0$, (b) $\kappa a/b = 3$, and (c) $\kappa a/b \to \infty$, respectively, for values of mass ratio ranging from 0 to ∞ and fixed permeability $\alpha = 2$. For any combination of $\kappa a/b$, and finite values of M/m and α, the electrophoretic mobility increases monotonically with the time from $t = 0$ to its steady state $t \to \infty$. Also note that the mobility is not increasing as rapidly as the velocity slip does. For constant values of $\nu t/a^2$, $\kappa a/b$ and α, the mobility is monotonically increasing as M/m decreases. We note that for thick and thin double layers and finite α, a heavier particle has a longer time-dependent duration than a lighter one in the development of the electrophoretic mobility. In the limiting case of $M/m \to \infty$, the mobility vanishes regardless of the values of $\kappa a/b$, α and $\nu t/a^2$. For any value of the mass ratio, it is interesting to observe that for thick double layer and a specified value of $\nu t/a^2$, the mobility function increases with the permeability parameter while for thin double layer it decreases as the permeability parameter increases. Finally, Fig. 4d exhibits the variation of the normalized electrophoretic mobility μ versus the permeability parameter α for different values of $\nu t/a^2$ and M/m with $\kappa a/b = 5$. It indicates that the maximum relative values of μ occur in the Stokes limit. For low permeability in the range of Darcian limit, $\mu(t)$ decreases rapidly to zero, regardless of $\nu t/a^2$ and M/m. The normalized electrophoretic mobility as a function of the non-dimensional elapsed time is also plotted for various values of $\kappa a/b$ and α in Fig. 5 for the cases of $M/m = 10$ and $M/m = 0$. For Stokes' flow ($\alpha = 0$), and when the double layer is relatively thin, the particle mobility decreases monotonically with a decrease in $\kappa a/b$ for fixed values of M/m and $\nu t/a^2$. On the other hand, for Brinkman flow ($\alpha > 0$) and for fixed values of M/m and $\nu t/a^2$, the mobility of the particle may decrease or increase; it depends strongly on the values of $\kappa a/b$. Figure 5 illustrates also that for fixed M/m and $\kappa a/b$, the time-dependent duration of the particle mobility is greater for the Stokes flow ($\alpha = 0$) than that of the Brinkman flow ($\alpha > 0$). Figure 6 shows plots of the normalized acceleration $(a^2/\nu)\mathrm{d}\mu/\mathrm{d}t$ of a spherical particle experiencing unsteady electrophoresis versus the dimensionless elapsed time $\nu t/a^2$ with M/m, $\kappa a/b$ and α as parameters. For both the Stokes and Brinkman flows ($\alpha \geq 0$) with the limiting case of $\kappa a/b = 0$ and for the entire range of M/m, as illustrated in Fig. 6a, the acceleration is a monotonic decreasing function of $\nu t/a^2$ and it is finite at the instant the electric field is applied. Again for both the Stokes and Brinkman flows and for the case with a thin double layer, but finite ($\kappa a/b = 3$) as indicated in Fig. 6b, the non-dimensional acceleration first increases with $\nu t/a^2$ from $t = 0$ to a maximum at a small finite value of $\nu t/a^2$ and then decreases with $\nu t/a^2$ monotonically. The vanishing of the initial acceleration in this case is a consequence of the zero velocity slip at the surface of the particle surface at $t = 0$. Once more for the cases of Stokes and Brinkman flows ($\alpha \geq 0$) and for the limiting case of $\kappa a \to \infty$ as indicated in Fig. 6c, the acceleration is a monotonic decreasing function of $\nu t/a^2$ and is infinite at the instant the electric field is applied. The infinite initial acceleration is a consequence to the finite velocity slip at the surface of the particle, which develops the movement of the particle, even at the time $t = 0$. For $\alpha \geq 0$ and fixed values of M/m and $\kappa a/b$, the acceleration of the particle decreases quickly after $\nu t/a^2$ is equal to about 0.125 and vanishes when $\nu t/a^2$ tends to infinity. As $M/m \to \infty$, the normalized acceleration is zero for the entire range of permeability parameter with all values of $\kappa a/b$. The acceleration also has unspecified behaviour for different values of the permeability parameter with fixed values of the mass density and Debye length parameters.

8. Conclusion

In this article, an expression for apparent velocity slip at the surface of a dielectric plane is first developed. This velocity slip is employed as a boundary condition to solve the electrophoretic motion of a dielectric spherical particle embedded in a porous medium under the unsteady Darcy–Brinkman model. Two related problems are then solved under the time-dependent Darcy–Brinkman equation applicable to the systems of a particle with a thin but finite double layer and of a particle with a thick double layer. Expressions for the electrophoretic mobility of the particle as functions of the relevant parameters are obtained for each

case. The present paper is an extension of the work of Keh and Huang [14] to the case of porous medium using Darcy's–Brinkman model for transient flow. Our study is also related to a recent work by Chiang and Keh [17] in which they used the cell model techniques and considered low values of particle volume fraction. The advantage of this investigation is to include all values of permeability from Stokes' clear fluids to Darcy's limit. Our results also cover the thin, but finite and thick electrophoretic double layers. The results indicate that the effect of permeability of the porous medium on the mobility is significant and interesting. However, our study gives useful understanding into the physical phenomena of the time-dependent reply of a dielectric particle to a quick action of a uniform electric field. The results show that the effect of the relaxation time for unsteady electrophoresis in general is negligible, regardless of the magnitude of the applied field, the value of the scalar zeta potential at the surface of the particle, the value of double layer thickness and the permeability of the medium. In fact, experimental data of the apparent velocity slip and the normalized electrophoretic mobility for porous medium would be required to compare our results.

References

[1] Reuss, F.F.: Sur un nouvel effet de l'électricité galvanique. Mem. Soc. Imp. Nat. Moscou **2**, 326–337 (1809)
[2] Russel, W.B., Saville, D.A., Schowalter, W.R.: Colloidal Dispersions. Cambridge Univ. Press, New York (1989)
[3] Dukhin, A.S., Goetz, P.J.: Ultrasound for Characterizing Colloids: Particle Sizing. Zeta Potential Rheology. Elsevier, Amsterdam (2002)
[4] Smoluchowski, M.: Contribution à la théorie de l'endosmose électrique et de quelques phénomènes corrélatifs. Bull. Int. Acad. Sci. Cracovie **8**, 182–200 (1903)
[5] Burgreen, D., Nakache, F.R.: Electrokinetic flow in ultrafine capillary slits. J. Phys. Chem. **68**, 1084–1091 (1964)
[6] Berli, C.L.A., Olivares, M.L.: Electrokinetic flow of non-Newtonian fluids in microchannels. J. Colloid Interface Sci. **320**, 582–589 (2008)
[7] Chang, C.C., Wang, C.Y.: Electro-osmotic flow in a sector microchannel. Phys. Fluids **21**, 042002 (2009)
[8] Zhao, C., Yang, C.: Advances in electrokinetics and their applications in micro/nano fluidics. Microfluid. Nanofluid. **13**, 179–203 (2012)
[9] Morrison, F.A.: Transient electrophoresis of an arbitrarily oriented cylinder. J. Colloid Interface Sci. **36**, 139–145 (1971)
[10] Ivory, C.F.: Transient electroosmosis: the momentum transfer coefficient. J. Colloid Interface Sci. **96**, 296–298 (1983)
[11] Keh, H.J., Tseng, H.C.: Transient electrokinetic flow in fine capillaries. J. Colloid Interface Sci. **242**, 450–459 (2001)
[12] Jian, Y., Yang, L., Liu, Q.: Time periodic electro-osmotic flows through a microannulus. Phys. Fluids **22**, 042001 (2010)
[13] Morrison, F.A.: Transient electrophoresis of a dielectric sphere. J. Colloid Interface Sci. **29**, 687–691 (1969)
[14] Keh, H.J., Huang, Y.C.: Transient electrophoresis of dielectric spheres. J. Colloid Interface Sci. **291**, 282–291 (2005)
[15] Chen, G.Y., Keh, H.J.: Start-up of electrokinetic flow in a fibrous porous medium. J. Phys. Chem. C **118**, 2826–2833 (2014)
[16] Chiang, C.C., Keh, H.J.: Transient electroosmosis in the transverse direction of a fibrous porous medium. Colloids Surf. A **481**, 577–582 (2015)
[17] Chiang, C.C., Keh, H.J.: Startup of electrophoresis in a suspension of colloidal spheres. Electrophoresis **36**, 3002–3008 (2015)
[18] Jones, E.H., Reynolds, D.A., Wood, A.L., Thomas, D.G.: Use of electrophoresis for transporting nano-iron in porous media. Ground Water **49**, 172–183 (2010)
[19] Pomès, V., Fernández, A., Houi, D.: Characteristic time determination for transport phenomena during the electrokinetic treatment of a porous medium. Chem. Eng. J. **87**, 251–260 (2002)
[20] Oyanader, M.A., Arce, P., Dzurik, A.: Design criteria for soil cleaning operations in electrokinetic remediation: hydrodynamic aspects in a cylindrical geometry. Electrophoresis **26**, 2878–2887 (2005)
[21] Riviere, J.E., Heit, M.C.: Electrically-assisted transdermal delivery. Pharm. Res. **14**, 687–697 (1997)
[22] Pyell, U.: Characterization of nanoparticles by capillary electromigration separation techniques. Electrophoresis **31**, 814–831 (2010)
[23] Calladine, C.R., Collis, C.M., Drew, H.R., Mott, M.R.: A study of electrophoretic mobility of DNA in agarose and polyacrylamide gels. J. Mol. Biol. **221**, 981–1005 (1991)
[24] Shi, Q., Jackowski, G.: One-dimensional polyacrylamide gel electrophoresis. In: Hames, B.D. (ed.) Gel Electrophoresis of Proteins: A Practical Approach, pp. 1–52. Oxford University Press, Oxford (1998)
[25] Magdeldin, S.: Gel Electrophoresis Principles and Basics. InTech, Rijeka (2012)

[26] Paillat, T., Moreau, E., Grimaud, P.O., Touchard, G.: Electrokinetic phenomena in porous media applied to soil decontamination. IEEE Trans. Dielectr. Electr. Insul. **7**, 693–704 (2000)
[27] Wu, Y.F., Chou, W.L., Yen, S.C.: Removal of mercury and methylmercury from contaminated soils by applying an electric field. J. Environ. Sci. Health A **35**, 1153–1170 (2000)
[28] Feng, J., Ganatos, P., Weinbaum, S.: Motion of a sphere near planar confining boundaries in a Brinkman medium. J. Fluid Mech. **375**, 265–296 (1998)
[29] Tsai, P., Huang, C.H., Lee, E.: Electrophoresis of a charged colloidal particle in porous media: boundary effect of a solid plane. Langmuir **27**, 13481–13488 (2011)
[30] Ingham, D.B., Pop, I.: Transport Phenomena in Porous Media II. Elsevier, Oxford (2002)
[31] Kaviany, M.: Principles of Heat Transfer in Porous Media, 2nd edn. Springer, New York (1995)
[32] Nabovati, A., Llewellin, E.W., Sousa, A.C.M.: A general model for the permeability of fibrous porous media based on fluid flow simulations using the lattice Boltzmann method. Compos. A **40**, 860–869 (2009)
[33] Vafai, K.: Handbook of Porous Media, 3rd edn. CRC Press, New York (2015)
[34] Neale, G., Epstein, M., Nader, W.: Creeping flow relative to permeable spheres. Chem. Eng. Sci. **28**, 1865–1874 (1973)
[35] Durlofsky, L., Brady, J.F.: Analysis of the Brinkman equation as a model for flow in porous media. Phys. Fluids **30**, 3329–3341 (1987)
[36] Sherief, H.H., Faltas, M.S., Saad, E.I.: Stokes resistance of a porous spherical particle in a spherical cavity. Acta Mech. **227**, 1075–1093 (2016)
[37] El-Sapa, S., Saad, E.I., Faltas, M.S.: Axisymmetric motion of two spherical particles in a Brinkman medium with slip surfaces, fluid. Eur. J. Mech. B Fluids **67**, 306–313 (2018)
[38] He, Y.Y., Lee, E.: Electrophoresis in concentrated dispersions of charged porous spheres. Chem. Eng. Sci. **63**, 5719–5727 (2008)
[39] Keh, H.J., Anderson, J.L.: Boundary effects on electrophoretic motion of colloidal spheres. J. Fluid Mech. **153**, 417–439 (1985)
[40] Tsay, R., Weinbaum, S.: Viscous flow in a channel with periodic cross-bridging fibres: exact solutions and Brinkman approximation. J. Fluid Mech. **226**, 125–148 (1991)
[41] Uematsu, Y.: Electrophoresis of electrically neutral porous spheres induced by selective affinity of ions. Phys. Rev. E **91**, 022303 (2015)
[42] Happel, J., Brenner, H.: Low Reynolds Number Hydrodynamics. Martinus Nijoff, The Hague (1983)
[43] Maribo-Mogensen, B., Kontogeorgis, G.M., Thomsen, K.: Comparison of the Debye-Hückel and the mean spherical approximation theories for electrolyte solutions. Ind. Eng. Chem. Res. **51**, 5353–5363 (2012)

E. I. Saad
Department of Mathematics, Faculty of Science
Damanhour University
Damanhûr
Egypt
e-mail: elsayedsaad74@yahoo.com;
elssaad@sci.dmu.edu.eg

M. S. Faltas
Department of Mathematics, Faculty of Science
Alexandria University
Alexandria
Egypt

(Received: August 14, 2017; revised: January 24, 2018)